LRP 658/00 January 2000

Enhanced thrid-order nonlinearity in semiconductors giving rise to 1 THz radiation

R. Brazis, R. Raguotis, Ph. Moreau,
M.R. Siegrist

accepted for publication in
Int. J. of Infrared and Millimeter Waves

ISSN 0458-5895

ENHANCED THIRD-ORDER NONLINEARITY IN SEMICONDUCTORS GIVING RISE TO 1 THz RADIATION

R. Brazis[1], R. Raguotis[1], Ph. Moreau[2] and M. R. Siegrist[3]

[1]Semiconductor Physics Institute, A.Go_tauto 11, 2600 Vilnius, Lithuania
[2]CE Cadarache DRFC/SCCP Bat 507. F-13108 St Paul les Durance, France
[3]JET-EFDA Close Support Unit, UKAEA Fusion, Culham Science Centre, Abingdon OX14 3DB, U.K.; permanent address: Centre de Recherche en Physique des Plasmas; Ecole Polytechnique Fédérale de Lausanne; PPB Ecublens, 1015 Lausanne; Switzerland

Abstract

Third harmonic generation (THG) efficiency is shown to be a greatly enhanced at the onset of inelastic scattering of electrons on optic phonons. Scaling experiments are performed on n-type InP at the pump wave frequency of 9.43 GHz at 80 K. Monte Carlo modeling is employed for scaling the effect to the 3rd harmonic frequency of 1 THz. The THG efficiency in n-type GaAs and InP as well as in the wurtzite phase of n-type InN and GaN compound crystals is compared to that in n-type Si. The efficiency maximum is found to weaken due to the quasi-elastic scattering on acoustic phonons and elastic scattering on ionized impurities. Nevertheless, the THG efficiency at 1 THz in InP crystals cooled down to liquid nitrogen temperatures is predicted to be 2 orders of magnitude higher than the reference value of 0.1% experimentally recorded up to now in n-type Si. ***Key words:*** *Frequency conversion; infrared optical materials, semiconductors, high power MM waves.*

1. Introduction

Our studies have been motivated by the need of a high power, high frequency radiation source for plasma diagnostic purposes [1]. One possible way to achieve this is by efficient frequency conversion of high-power gyrotron radiation in nonlinear materials. The desired frequency of >1 THz could, for example, be achieved from third harmonic generation using a pump frequency of >333 GHz, where high power gyrotrons do not exist at present, but where their development could be envisaged. While optically-pumped far-infrared lasers are also candidates, their short pulse duration (typically 1 μs) precludes them from the plasma diagnostic application considered. However, they have been used as primary sources for the feasibility study of frequency multiplication in nonlinear media. If the radiation of a gyrotron could be converted with reasonable efficiency (~10%) to higher harmonics, the problem would be solved.

Frequency conversion simulation in n-type Si crystals by means of a Monte Carlo technique compared to experimental data has allowed us to explain the 3rd harmonic intensity saturation at pumping intensities up to 2 MW/cm^2 at the fundamental frequency of 443 GHz [2]. N-type Si at room temperature turned out to be not the best possible choice with a power conversion efficiency not exceeding about 0.1%. While this is clearly insufficient for plasma diagnostic purposes, the 3rd harmonic radiation produced in silicon is found to be a source of precise information on material parameters governing their behavior at high power levels [3]. Cooling the crystals from 300 K down to 80 K has been predicted to result in a significant enhancement of the third harmonic gen-

eration (THG) efficiency at high pump wave amplitudes [4]. On the other hand, recent modeling data at relatively low amplitudes for the pump wave frequency of 333 GHz revealed a pronounced maximum of the THG efficiency in GaAs and InP related to the inelastic process of optic phonon emission by electrons [5]. However, powerful pump wave sources operating at such a high frequency are not yet available, and the predictions need to be verified in scaling experiments.

In this work we start with scaling experiments in the X-band aiming at obtaining evidence for the enhancement of the THG efficiency due to the onset of optic phonon emission (Section 2). Employing a Monte Carlo technique for further extrapolation to higher frequencies we elucidate the importance of electron scattering on ionized impurities (Section 3). Focusing our attention on the optic phonon emission as a most efficient electronic mechanism of THG, we extend the Monte Carlo modeling to the wurtzite phase of InN and GaN (Section 4). In conclusion, we discuss future THG experiments in the terahertz range.

2. Scaling experiments

We have performed scaling experiments at T=80 and 300 K using a magnetron emitting at 9.43 GHz a power of up to 70 kW. A waveguide tapered to the reduced cross-section of 3.4×7.2 mm has been used as a stop-filter of the fundamental wave. The samples have been positioned in the waveguide cross-section of 10×23 mm at the maximum of the pump wave electric field [6]. The forward-emitted 3rd harmonic wave efficiency in InP at 80 K is a maximum at the pump power of 1.5-2 kW (Fig. 1a).

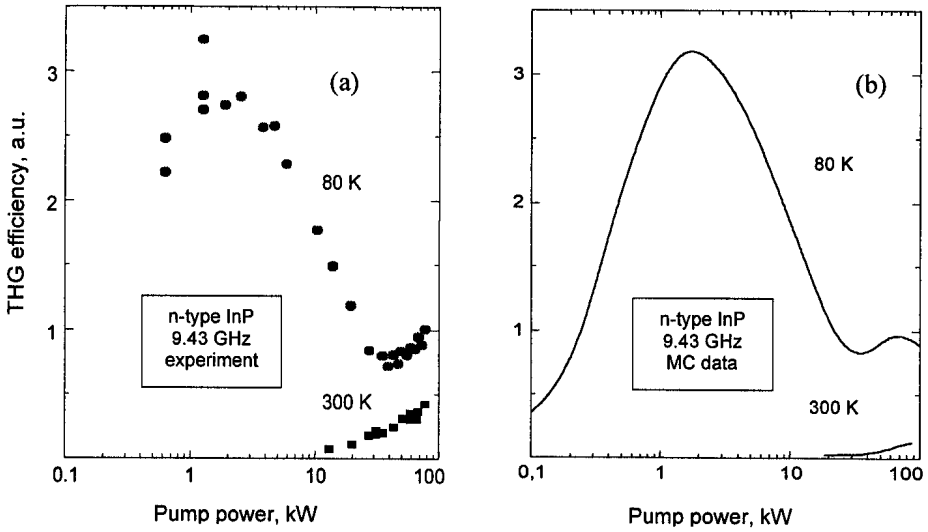

Fig. 1. (a) - Experimental THG efficiency dependence on the pump wave power in n-type InP; epitaxial sample is positioned in the 10×23 mm waveguide cross-section plane, the layer thickness is 7μm, the electron density is $n=4\times10^{14}$ cm^{-3}, and the insulating InP substrate thickness is 433μm; (b) – Monte Carlo modeling data on the electronic efficiency η_3 (Eq.1) vertically scaled so as to fit the experiment.

The efficiency starts to increase again at the pump power exceeding 30 kW, indicating the onset of the second maximum. A reasonable agreement between the experiment and the Monte Carlo modeling data can be achieved taking into account a quite high density of ionized impurity atoms of $N_i=10^{16}$ cm^{-3} (Fig. 1b). The total ionized impu-

rity density in our experimental samples was not specified, but it was certainly not less than the above value because of doping compensation and other point defects. This could in part explain the observed low efficiency that has not been otherwise optimized. Another destructive factor is the interference of the 3rd harmonic radiation emitted by different parts of the sample because the 3rd harmonic phase is sensitive to the pump wave amplitude [4] which is quite non-uniform in the rectangular waveguide.

The conclusion drawn from the experiments is that the efficiency of the 3rd harmonic generation is a maximum when the conditions of the optic phonon emission are fulfilled. This is an essential result confirming the details of the model and allowing extrapolation to the target frequency of 1 THz.

2. Modeling

We determine the electronic efficiency of third harmonic generation by means of a Monte Carlo technique aiming at a comparison of the most promising A^3B^5 compounds with Si crystals. We account for the joint action of several mechanisms contributing to the nonlinearity. These are the nonparabolicity of the electron energy dependence on momentum (causing an effective mass variation analogous to relativistic effects of free electrons), the electron transfer between multiple energy valleys differing by the effective mass, and the inelastic scattering of electrons at the onset of phonon generation. Specifically, we consider the question to what extent the nonlinearities are affected by randomizing electron scattering on thermal phonons and ionized impurities in crystals.

The Monte Carlo code is designed in a standard algorithm to provide the time dependence of the drift velocity of electrons. In order to reduce the statistical scatter, the number of electrons is chosen for the simulation between 5×10^5 at low amplitudes and 10^4 at high amplitudes depending on material parameters and temperatures. The Fourier transform of this velocity gives the amplitude and phase of the harmonic current that is the source of radiation emitted by the sample. The total efficiency depends both on the details of the nonlinear set-up and on the inherent electronic efficiency η_3 that is [4]:

$$\eta_3 = \frac{I_3}{I_1^{inc}} = Kn^2d^2\left|\frac{V_3}{E_1}\right|^2, \qquad (1)$$

where I_3 is the forward-emitted 3rd harmonic wave intensity, I_1^{inc} is the incident pump wave intensity, K is a coefficient independent of the material parameters except for the lattice dielectric constant provided that the carrier contribution to the dielectric constant is low compared to the lattice contribution, n is the electron density, d is the sample thickness assumed to be small compared to the wavelength, V_3 is the 3rd harmonic drift velocity amplitude, and E_1 is the pump wave amplitude in the sample.

For the electron motion in n-type Si six ellipsoidal nonparabolic X-valleys are considered (Tab.1). One type of acoustic phonons in the elastic approximation and equipartition is accounted for the intravalley scattering, whereas intervalley scattering which requires high-momentum phonons is modeled using a set of 6 types of phonons. The values of constants used in the modeling are are similar to these in Ref. [7] (Tab. 2). Other parameters used in our model are the crystal density of 2.33 g/cm^3, the longitudinal sound velocity of 9×10^5 cm/s, the acoustic deformation potential of 9 eV [8]. Direct comparison of simulation results obtained using these parameters with experimental data of third harmonic generation at room temperature has been successful [3].

Table 1. Electron parameters in Si

Valleys	*X*
Number of valleys	*6*
Nonparabolicity coef., eV^{-1}	*0.5*
Electron effective mass:	
longitudinal, m_l/m_o	*0.9*
transverse, m_t/m_o	*0.192*

Table 2. Phonon parameters in Si

Type	*ε, meV*	*D_{ij}, GeV/cm*
f	*19*	*0.03*
f	*47.4*	*0.2*
f	*59*	*0.2*
g	*12*	*0.05*
g	*18.5*	*0.08*
g	*62*	*1.1*

The band structure of InP is similar to GaAs with approximately 1.5 times higher separation between the Γ and X, and Γ and L valleys (Tab. 3).

Table 3. GaAs and InP crystal parameters (close to these in Ref. [9])

Compound	*GaAs*			*InP*		
Density, g/cm^3	*5.32*			*4.8*		
Longit. sound velocity, 10^5 cm/s	*5.24*			*5.13*		
Static dielectric constant	*12.8*			*12.35*		
Optic dielectric constant	*10.9*			*9.52*		
Energy gap at 300 K, eV [8]	*1.429*			*1.344*		
Energy valley	*Γ*	*L*	*X*	*Γ*	*L*	*X*
Number of valleys	*1*	*4*	*3*	*1*	*4*	*3*
Energy separation, eV	*-*	*0.33*	*0.52*	*-*	*0.54*	*0.775*
Nonparabolicity coef., eV^{-1}	*0.69*	*0.65*	*0.36*	*0.83*	*0.23*	*0.38*
Electron effective mass, m_0	*0.063*	*0.23*	*0.43*	*0.078*	*0.26*	*0.325*
Acoustic def. potential, eV	*8*	*8*	*8*	*8*	*14.5*	*6.5*
Optic phonon energy, meV	*35*	*35*	*35*	*43*	*43*	*43*
Intervalley phonon coupling constants and energy	*D_{ij}, GeV/cm*		*ε_{ij}, meV*	*D_{ij}, GeV/cm*		*ε_{ij}, meV*
ΓL	*1*		*26*	*1*		*27.8*
ΓX	*1*		*26*	*1*		*29.9*
LL	*1*		*26*	*1*		*29*
LX	*0.9*		*26*	*0.9*		*29.3*
XX	*0.9*		*26*	*0.9*		*29.9*

The intervalley phonon energies and coupling constants of InP do not differ much from those in GaAs but the optic phonon energy, as well as the effective mass of electrons in the Γ valley, are 1.25 times higher in InP than in GaAs. We have performed calculations for the materials at lattice temperatures of 300 K and 80 K and compared them with the room temperature data of silicon where experimental results on the THG exist [3]. The THG efficiency, which is proportional to the square of the 3rd harmonic drift velocity amplitude ratio to the pumping wave field amplitude given by Eq. (1), is significantly higher when the crystal is cooled down to liquid nitrogen temperatures. All the materials are expected to exhibit a maximum efficiency at certain values of pump wave amplitude. At very low field amplitudes the drift response is linear causing the THG efficiency to approach zero. At high field amplitudes electrons access high mean energy compared to that lost for phonon emission, the scattering becomes randomizing again, and the 3rd order non-linearity decreases. These conclusions supported by Monte Carlo modeling contradict early expectations of a constant 3rd order non-linear susceptibility $\chi_{(3)}$ [10]. The initially cubic law of the 3rd harmonic output intensity $I_3 \propto \chi_{(3)}^2 I_1^3$ is subjected to saturation and even to a decrease with the rise of the pump wave power. These main features of modeling results are summarized in Fig. 2 showing the existence of optimum conditions for the 3rd harmonic generation. Electronic efficiency in n-type Si is a maximum at a pump wave amplitude inside the material of around 20 kV/cm at the

temperature of 300 K (Fig.2). The maximum is related to the onset of phonon-assisted transfer of electrons between equivalent ellipsoidal energy valleys that are differently oriented in momentum space. In GaAs electron transfer from the Γ valley to the upper L and X valleys bring about a maximum efficiency around 10 kV/cm, whereas in InP the analogous maximum is at pump wave amplitudes slightly above 25 kV/cm. This peculiarity has already been observed in THG modeling at high electric field amplitudes [4]. By extending the modeling to lower amplitudes [5] we have obtained a much more pronounced additional maximum of THG efficiency which manifests itself in GaAs and InP at low temperatures. It is by two orders of magnitudes higher than that in n-type Si.

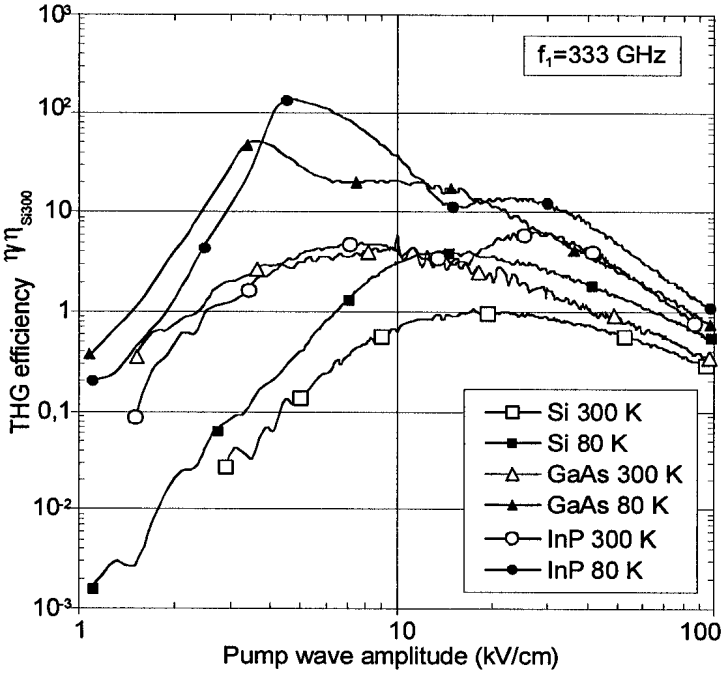

Fig. 2. THG efficiency in pure n-type Si, GaAs and InP normalized to the maximum efficiency of n-type Si at T = 300 K as function of the pump field amplitude. Materials and temperatures, as well as the fundamental frequency, are shown in the figure. Each curve consists of typically 175 points, and the undulation represents statistical scatter of the Monte Carlo simulation data. The points marked by symbols are given for trace identification.

Comparing the data for GaAs and InP, one can notice a correlation between the lower-field maximum position and the optical phonon energy. Therefore we attribute tentatively the additional maximum of THG efficiency to the inelastic scattering of electrons on polar optic phonons. It does not take place in Si crystals which lack a first order electric dipole related to optic phonon modes.

When the lattice temperature is T = 300 K then the effect of inelastic scattering of electrons by optic phonons is smeared out by randomizing scattering on other types of phonons. Other randomizing mechanisms like the ionized impurity scattering reduce the maximum at low temperatures, as well. This is shown by means of the Monte Carlo code modified so as to include the effect of ionized impurities using the Brooks-Herrings approximation [11]. The ionized impurity scattering turned out to be highly destructive at frequencies of the order of 10 GHz but in the high frequency range it does not reduce the maximum by more than a factor of 2 (Fig. 3).

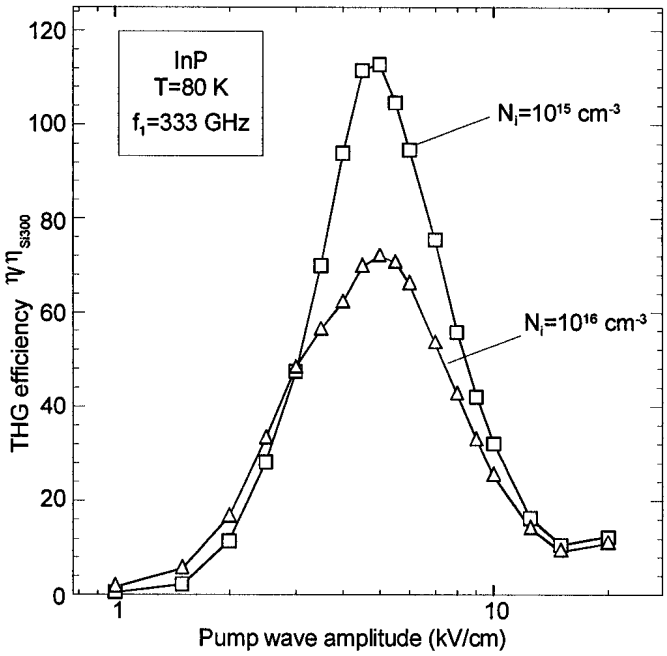

Fig. 3. THG efficiency as function of pump wave amplitude in n-type InP at 80 K for two different impurity concentrations at the pump wave frequency of 333 GHz. The ionized impurity concentration is shown in the figure.

The requirements for the sample doping turn out to be considerably relaxed at high pumping frequencies. This encouraged us to check the electronic nonlinearity in other crystals with considerably different optic phonon energies and higher separation between the energy valleys.

Among the variety of possibilities we have chosen GaN and InN compound crystals. They have recently attracted much attention as materials for blue lasers, as well as high-power microwave electronics because of their large energy gap preventing the avalanche breakdown. The compounds are known to crystallize both in zincblende and wurtzite phases but the material parameters are not yet well known. We have chosen the wurtzite modification where the drift current of electrons has already been considered in high DC electric fields [12]. The material parameters are presented in Tab. 4.

With the Monte Carlo code modified so as to include electron scattering on the piezoelectric potential relevant in these materials, we have obtained the results on the THG efficiency presented in Fig. 4. The maximum electronic efficiency of the 3rd harmonic generation related to the optic phonon generation is at E_1=8 kV/cm in InN and at 12 kV/cm in GaN.

Table 4. Wurtzite type crystal parameters (close to these in Ref.[12]).

Compound	*GaN*			*InN*		
Density, g/cm³	*6.15*			*6.81*		
Sound velocity, 10^5 cm/s:						
longitudinal	*6.56*			*6.24*		
transverse	*2.68*			*2.55*		
Static dielectric constant	*8.93*			*15.3*		
Optic dielectric constant	*5.35*			*8.4*		
Energy gap, eV	*3.39*			*1.89*		
Energy valley	*Γ_1*	*L-M*	*Γ_2*	*Γ_1*	*A*	*Γ_2*
Number of valleys	*1*	*6*	*1*	*1*	*4*	*3*
Energy separation, eV	*-*	*2.0*	*2.2*	*-*	*2.2*	*2.6*
Nonparabolicity coef., eV^{-1}	*0.189*	*0.067*	*0.029*	*0.419*	*0.088*	*0.36*
Electron effective mass, m^*/m_0	*0.2*	*0.4*	*0.6*	*0.11*	*0.4*	*0.6*
Acoustic deform. potential, eV	*8.3*			*7.1*		
Optic phonon energy, meV	*91.2*			*89*		
Piezoelectr. constant, C/cm^2	*3.75×10^{-5}*			*3.75×10^{-5}*		
Intervalley coupl. const., GeV/cm	*1*			*1*		
Intervalley phonon energy, meV	*91.2*			*89*		

The THG efficiency maximum in InN turns out to be somewhat higher than that in InP at the same impurity concentration of 10^{16} cm^{-3}. The other maximum related to the electron transfer to upper valleys is at much higher field amplitudes not considered here.

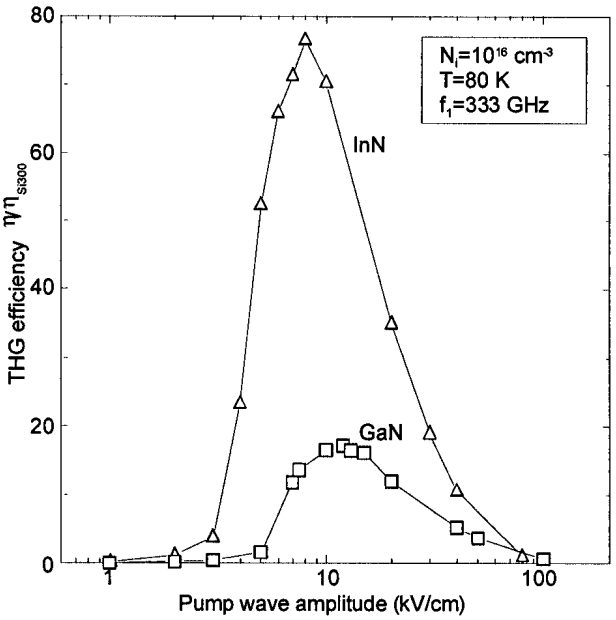

Fig. 4. THG efficiency in n-type GaN and InN.

The impurity concentration decrease down to $10^{15}cm^{-3}$ is found to result in an enhancement of the maximum efficiency in InN by 25% only. The lower sensitivity of the electron drift velocity in the nitrides to the presence of ionized impurities has been no-

ticed in the steady state electric fields, as well [13]. Gallium nitride seems to be inferior as far as the 3rd harmonic generation is considered (Fig.4). It should be remarked, however, that the conclusion is tentative because the zincblende phase of GaN exhibits highly nonlinear velocity vs electric field characteristics at the steady electric field. This has been predicted on the basis of Monte Carlo simulation including full zone band structure [14].

One can notice in Fig. 2 that the value of the pump wave amplitude at the additional maximum position in InP is at higher amplitudes than in GaAs. Analyzing the data in Figs. 2-4 with the material parameters given in Tabs. 3 and 4 one can see that the maximum position correlates with the optic phonon energy. Several other processes make the correlation weak. The correlation is improved if one accounts for both the optic phonon energy and the effective mass at the bottom of the conduction band. Such an account implies energy and momentum conservation. Neglecting the nonparabolicity and other scattering except the optic phonon emission, the integral of the equation of motion gives the value of $p=eE_1/\omega_1$ for the electron momentum acquired in a quarter period of the pump wave. If the electron kinetic energy $p^2/2m^*m_0$ is equal to the optic phonon energy ε_{opt} then the optic phonon is emitted and electron momentum is lost. This consideration of the optic phonon emission gives the threshold amplitude of

$$E_1^{th} = \omega_1 \sqrt{2m^* m_0 \varepsilon_{opt} / e^2} \,. \tag{2}$$

The threshold values obtained in this way are somewhat lower than the MC data on the position of the maximum electronic efficiency of the 3rd harmonic generation (Fig. 5).

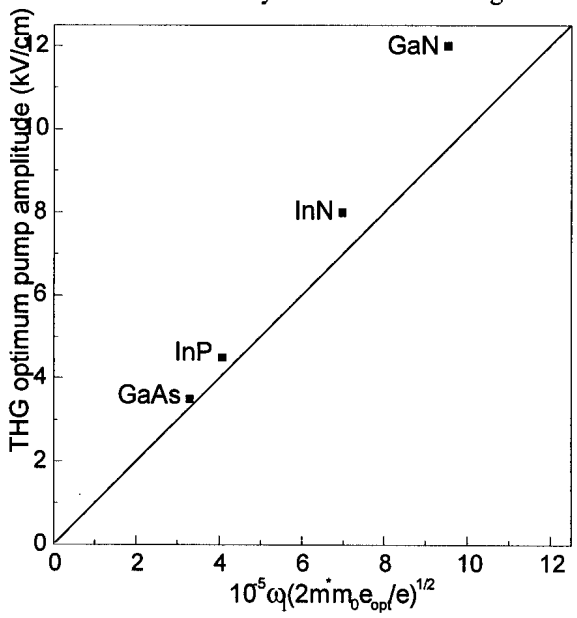

Fig. 5. Correlation between the Monte Carlo data on the THG efficiency maximum position (dots) and the threshold amplitude for the emission of optic phonons (solid line); here the phonon energy is expressed in eV. T=80 K, f_1=333 GHz.

4. Conclusion

In conclusion, optic phonon emission by electrons in A_3B_5 compound crystals at low temperatures is shown to give rise to a resonance-like enhancement of the electronic efficiency of the third harmonic generation at certain values of the pump wave intensity.

The predicted THG efficiency exceeds the values experimentally observed up to now in n-Si in the range of 1 THz by two orders of magnitude. Electron scattering on ionized impurities is shown to be highly destructive for the THG efficiency in gigahertz range whereas it is not as important in the terahertz frequency range because the efficiency maximum shifts to higher amplitudes with the rise of pump wave frequency. Electrons remain then for a shorter time in the low energy range thus making the impurity scattering less probable. This is a guideline for the next experimental step using a gyrotron operating at 118 GHz as a pump wave source. It must be emphasized that the maximum efficiency exceeds that in silicon in quite pure InP with the total ionized impurity density significantly less than 10^{15} cm^{-3}. We have focused our attention on the electronic efficiency only, leaving open other related problems of nonlinear optics. The 3rd harmonic phase dependence on the local amplitude of the pump wave demands careful selection of structures to further enhance the 3rd harmonic output both by the fundamental and the harmonic wave phase velocity matching and the input pump wave phase and amplitude control.

Our scaling experiments confirming the enhancement of THG efficiency at the onset of optical phonon emission provide a guideline for an optimum optical set-up. If one aims to optimize the THG output power in order to operate at the point of maximum efficiency, InP and InN seem to be superior. The low-temperature operation is favorable both for obtaining a high THG intensity and for the heat transfer from the nonlinear sample.

Acknowledgements: This work was partially supported by the Swiss National Science Foundation.

References

1. M. R. Siegrist, H. Bindslev, R. Brazis, D. Guyomarc'h, J. P. Hogge, Ph. Moreau, R. Raguotis, Infrared Physics and Technology, **40**, p. 247 (1999).
2. M. Urban, M. R. Siegrist, L. Asadauskas, R. Raguotis, and R. Brazis, Lithuanian J. Phys. **35**, p. 430 (1995).
3. M. Urban, M. R. Siegrist, L. Asadauskas, R. Raguotis, and R. Brazis, Appl. Phys. Lett. **69**, p. 1776 (1996).
4. R. Brazis, R. Raguotis and M. R. Siegrist, J. Appl. Phys. **84**, p. 3474 (1998).
5. R. Brazis, R. Raguotis, Ph. Moreau and M. R. Siegrist, in: The 23rd Int. Conf. IR and MM Waves, Colchester, September 7-11, 1998, Conference Digest, T.J. Parker and S.P.R. Smith, Eds., Univ. Essex, 1998, p. 280-281.
6. Ph. Moreau, M. R. Siegrist, R. Brazis and R. Raguotis, Material Science Forum, **297-298**, p. 315 (1999).
7. R. Brunetti, C. Jacoboni, T. Nava, L. Reggiani, G. Bosman and R. J. Zijlstra, J. Appl. Phys. **52**, p. 6713 (1981).
8. A. Dargys, J. Kundrotas. *Handbook on physical properties of Ge, Si, GaAs and InP, Sci. and Encyclopedia Publishers, Vilnius, 1994, 266 p.*
9. K. Brennan and P. K. Hess, Solid State Electronics, **25**, p. 589 (1982).
10. A. Mayer and F. Keilmann, Phys. Rev. **B33**, p. 6962 (1989).
11. B. Ridley, *Quantum Processes in Semiconductors, University Press, Oxford, 1982.*
12. S. K. O'Learly, B. E. Foutz, M. S. Shur, and U. V. Bhapkar, J. Appl. Phys. **83**, p. 826 (1998).
13. M. S. Shur, Solid-State Electronics, **42**, p. 2131 (1998).
14. J. Kolník, Í. H. O_uzman, K. F. Brennan, R. Wang, P. P. Ruden, and Y. Wang, J. Appl. Phys. **78**, p. 1033 (1995).